Systems/Circuits

A Resting-State Functional MR Imaging and Spectroscopy Study of the Dorsal Hippocampus in the Chronic Unpredictable Stress Rat Model

Ricardo Magalhães,[1,2] Ashley Novais,[1,2] David A. Barrière,[3,4] Paulo Marques,[1,2] Fernanda Marques,[1,2] João C. Sousa,[1,2] João J. Cerqueira,[1,2] Arnaud Cachia,[4,5] Therese M. Jay,[4] Michel Bottlaender,[3] Nuno Sousa,[1,2,6] Sébastien Mériaux,[3] and Fawzi Boumezbeur[3]

[1]Life and Health Sciences Research Institute (ICVS), School of Medicine, University of Minho, 4710-057 Braga, Portugal, [2]ICVS/3B's-PT Government Associate Laboratory, 4710-057 Braga/Guimarães, Portugal, [3]NeuroSpin, CEA, Université Paris-Saclay, 91190 Gif-sur-Yvette, France, [4]Inserm U894, Center for Psychiatry and Neurosciences, Université Paris-Descartes, 75014 Paris, France, [5]CNRS U8240, LaPsyDÉ, Université Paris-Descartes, 75005 Paris, France, and [6]Clinic Academic Center, Braga, 4710-243 Braga, Portugal

Exposure to chronic stress leads to an array of anatomical, functional, and metabolic changes in the brain that play a key role in triggering psychiatric disorders such as depression. The hippocampus is particularly well known as a target of maladaptive responses to stress. To capture stress-induced changes in metabolic and functional connectivity in the hippocampus, stress-resistant (low-responders) or -susceptible (high-responders) rats exposed to a chronic unpredictable stress paradigm (categorized according to their hormonal and behavioral responses) were assessed by multimodal neuroimaging; the latter was achieved by using localized ^{1}H MR spectroscopy and resting-state functional MRI (fMRI) at 11,7T data from stressed ($n = 25$) but also control ($n = 15$) male Wistar rats.

Susceptible animals displayed increased GABA–glutamine (+19%) and glutamate–glutamine (+17%) ratios and decreased levels of macromolecules (−11%); these changes were positively correlated with plasma corticosterone levels. In addition, the neurotransmitter levels showed differential associations with functional connectivity between the hippocampus and the amygdala, the piriform cortex and thalamus between stress-resistant and -susceptible animals. Our observations are consistent with previously reported stress-induced metabolomic changes that suggest overall neurotransmitter dysfunction in the hippocampus. Their association with the fMRI data in this study reveals how local adjustments in neurochemistry relate to changes in the neurocircuitry of the hippocampus, with implications for its stress-associated dysfunctions.

Key words: fMRI; functional connectivity; hippocampus; MRS; resistance and susceptibility; stress

Significance Statement

Chronic stress disrupts brain homeostasis, which may increase the vulnerability of susceptible individuals to neuropsychiatric disorders such as depression. Characterization of the differences between stress-resistant and -susceptible individuals on the basis of noninvasive imaging tools, such as magnetic resonance spectroscopy (MRS) and magnetic resonance imaging (MRI), contributes to improved understanding of the mechanisms underpinning individual differences in vulnerability and can facilitate the design of new diagnostic and intervention strategies. Using a combined functional MRI/MRS approach, our results demonstrate that susceptible- and non-susceptible subjects show differential alterations in hippocampal GABA and glutamate metabolism that, in turn, associate with changes in functional connectivity.

Introduction

The multiple levels at which stress impacts the brain is well documented (Cameron et al., 1995; Sousa et al., 2000; Czéh et al., 2001; Brown et al., 2005; Grønli et al., 2007; Dias-Ferreira et al., 2009; Popoli et al., 2011; Anacker et al., 2016; Magalhães et al., 2017, 2018; Gray et al., 2018). Although maladaptive neuro-

Received Aug. 13, 2018; revised Jan. 21, 2019; accepted Jan. 29, 2019.

Author contributions: R.M., A.N., F.M., J.C.S., J.J.C., A.C., T.M.J., M.B., N.S., S.M., and F.B. designed research; R.M., A.N., D.A.B., T.M.J., M.B., S.M., and F.B. performed research; R.M., A.N., P.M., N.S., and F.B. analyzed data; R.M. and N.S. wrote the first draft of the paper; R.M., A.N., D.A.B., P.M., F.M., J.C.S., J.J.C., A.C., T.M.J., M.B., N.S., S.M., and F.B. edited the paper; R.M., A.N., D.A.B., P.M., F.M., J.C.S., J.J.C., A.C., T.M.J., N.S., S.M., and F.B. wrote the paper.

This work is part of the Sigma project (FCT-ANR/NEU-OSD/0258/2012) cofinanced by the French ANR (Agence National pour la Recherche, APP Blanc International II 2012), the Portuguese FCT (Fundação para a Ciência e

structural and metabolic responses to prolonged stress associate strongly with the emergence of neuropsychiatric disorders (Sousa, 2016), our understanding of why some individuals are more susceptible than others to developing stress-related disorders of the brain remains poor. Noninvasive techniques such as magnetic resonance imaging (MRI) and magnetic resonance spectroscopy (MRS) offer unprecedented opportunities to concomitantly assess brain anatomy, function and metabolism in stressed subjects. To date, only a few studies have used either *in vivo* MRS to study changes in neurometabolism (Czéh et al., 2001; Delgado y Palacios et al., 2011; Xi et al., 2011; Hemanth Kumar et al., 2012) or resting-state functional MRI (rs-fMRI) to explore how stress impacts on functional networks in rodent models (Henckens et al., 2015; Magalhães et al., 2018; Nephew et al., 2018). Briefly, stress-induced changes in the concentrations of *N*-acetylaspartate (NAA; Xi et al., 2011), glutamate (Glu; Delgado y Palacios et al., 2011; Hemanth Kumar et al., 2012), glutamine (Gln), GABA, taurine, myo-inositol (Hemanth Kumar et al., 2012), and *N*-acetylaspartatyl-glutamate (Delgado y Palacios et al., 2011) were reported after *in vivo* MRS analysis of the hippocampus and prefrontal cortex. Those findings were complemented by *ex vivo* studies (Knox et al., 2010; Llorente et al., 2012; Perrine et al., 2014). Notably, the direction of changes were often found to be inconsistent between studies (possibly because of differences in the stress and MRS protocols), and only one of those studies (Delgado y Palacios et al., 2011) attempted to examine interactions between the response to stress and metabolic changes.

A central question in contemporary stress research concerns the biological mechanisms underlying variable responses made by individual humans and animals after exposure to stress. What characterizes "stress resistance"? What underpins susceptibility to the disruptive effects of stress, including predisposition to psychiatric disorders? The value of MRS and MRI in understanding the role of altered glutamatergic and GABAergic metabolism in the pathophysiology of depression in patients has been demonstrated previously (Sanacora et al., 2002; Abdallah et al., 2014, 2018). In the present study in rats, we used the chronic unpredictable stress paradigm to mimic some of the phenotypic features of depression (Bondi et al., 2008) to further explore the neurobiological basis of resilience to stress using MRI and MRS. Subsequently, rats were examined by MRS and MRI to obtain measures of metabolic activity and functional connectivity (FC) in their hippocampus; joint monitoring of these parameters has been achieved in only a limited number of recent studies (Haag et al., 2015; Ip et al., 2017; Chen et al., 2018). The experiments reported in the current work extend our earlier report on FC and structural changes in the brain of stressed rodents (Magalhães et al., 2018). Specifically, the previous analysis revealed changes in the connection between the dorsal hippocampus and the prefrontal cortex when contrasting control and stressed animals. Hippocampal circuits have often been suggested to have a central role in the development of stress-related dysfunctions. Stress is known to interfere with memory by interrupting hippocampal-fronto-cortical connectivity (Doyère et al., 1993; Jay et al., 2004; Cerqueira et al., 2007). Stress triggers fear, anxiety, and dysregulation of glucocorticoid-negative feedback within the limbic-hypothalamic-pituitary-adrenal axis (LHPA) by disrupting information relay between the hippocampus and amygdala, bed nucleus of the stria terminalis and hypothalamus (Jacobson and Sapolsky, 1991; Akirav and Richter-Levin, 1999; Pitkänen et al., 2000; Richter-Levin and Akirav, 2000). Building on this background, the current work couples MRS and rs-fMRI to establish whether stress-susceptible and stress-resistant animals exhibit distinct neurochemical and FC signatures.

Materials and Methods

Experimental design and statistical analysis. A set of 40 male Wistar rats, aged 8 weeks, (Janvier Labs) was housed, in pairs, under standard laboratory conditions (light cycle from 07:00 A.M. to 07:00 P.M.; temperature 22°C and relative humidity 55%) with *ad libitum* access to food and water, unless otherwise specified. The animals were divided into two subgroups: controls ($n = 15$) and experimental ($n = 25$). The latter group was exposed for 21 days to a chronic unpredictable stress (CUS) protocol. In this protocol, animals were stressed daily to a randomly assigned stressor (1 h overcrowding, 1 h in a wet cage with water at 18°C, 1 h restraint, 15 min exposure to hot air, or inversion of the light/dark cycle over a weekend). Control animals were gently handled on a daily basis. This CUS protocol has been shown to induce a phenotype that includes elevated plasma levels of corticosterone, and anxiety and altered stress-coping behavior (Magalhães et al., 2018). All animal experiments were performed in strict accordance with the recommendations of the European Community (2010/63/EU), the French (Decree No. 2013-118) and Portuguese legislation (Decreto-Lei No. 113/2013) on the use and care of laboratory animals; procedures were approved by the Ministère de l'Enseignement Supérieur et de la Recherche (APAFIS 1080) and the regional committee on animal ethics (CETEA/CEA/DSV IdF, protocol ID 13-023). The work presented here is a continuation of our previous study (Magalhães et al., 2018), focusing on a subset of animals, exploring MRS data and the functional circuits of the hippocampus. Metabolite concentrations were compared first between the two experimental groups (control and CUS) and then between the two stress clusters (low and high responders) using independent samples *t* tests. The metabolites found to be different were further explored via correlation analyses with the individual stress assessment parameters through a Pearson correlation analysis conducted using SPSS v25 (https://www.ibm.com/analytics/data-science/predictive-analytics/spss-statistical-software; RRID:SCR_002865).

The impact of the stress exposure (comparing controls to CUS animals) and of the response to stress (comparing Low- and High-responders) on the FC of the hippocampus was tested through two-sample *t* tests using MATLAB v7 (MathWorks; RRID:SCR_001622). Association between the GABA/Gln and Glu–Gln ratios and the FC of the hippocampus were explored by testing the interaction effect of the ratios and the response cluster on the FC of the hippocampus between the High- and Low-responder groups using MATLAB. Analysis was done using the general linear model using FC as the dependent variable, the cluster-by-neurotransmitter interaction as variable-of-interest and the individual terms as co-variables.

The normality of all variables was confirmed through its skewness (ranging from −0.5 to 1.3) and kurtosis (ranging from −0.4 to 3.1). Three subjects (2 CUS and 1 control) were identified as outliers in their behavior scores (diverging by >3 SD from the group average) and excluded from the analysis. Furthermore, one control was found to have spectra with insufficient quality and for that reason was also excluded, resulting in 36 animals (23 CUS and 13 Control) used in the first part of the analysis. All raw statistics values, significances (with results considered significant at $p < 0.05$), measures of effect sizes (Hedges *g*) and

Tecnologia) and by the project NORTE-01-0124-FEDER-000021, supported by the Portuguese North Regional Operational Program (ON.2–O Novo Norte), under the National Strategic Reference Framework (QREN) through the European Regional Development Fund (FEDER), by the project NORTE-01-0145-FEDER-000013, supported by the Northern Portugal Regional Operational Programme (NORTE 2020), under the Portugal 2020 Partnership Agreement through the FEDER as well as the Competitiveness Factors Operational Programme (COMPETE), and the Foundation for Science and Technology (FCT) under the scope of the project POCI-01-0145-FEDER-007038, and performed on a platform of the France Life Imaging network partly funded by Grant ANR-11-INBS-0006; R.M. was supported by Grant PDE/BDE/113604/2015 from the PhD-iHES program of the School of Medicine of Universidade do Minho. We thank Douglas L. Rothman, Grame F. Mason, and Osborne Almeida for their feedback.

The authors declare no competing financial interests.

Correspondence should be addressed to Ricardo Magalhães at id5832@alunos.uminho.pt.

https://doi.org/10.1523/JNEUROSCI.2192-18.2019

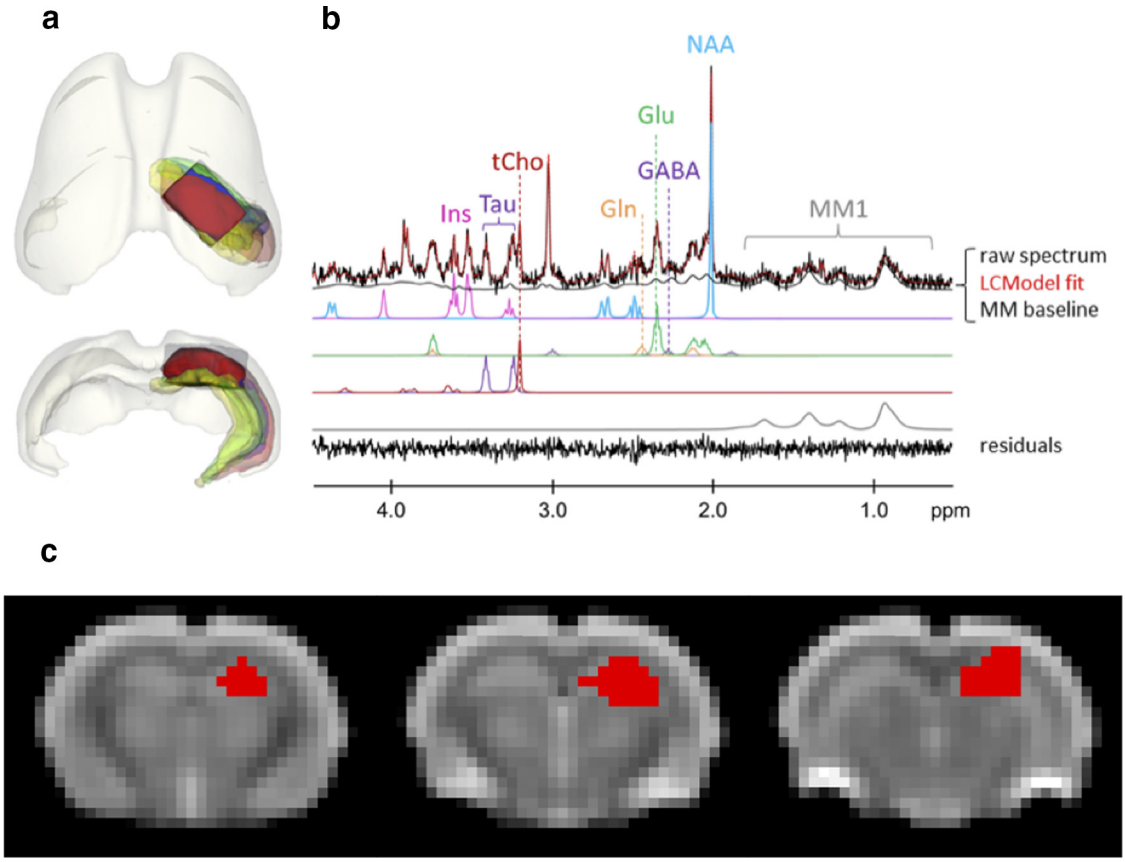

Figure 1. ***a***, Positioning of the MRS voxel over the right dorsal hippocampus. White mesh represents the rat corpus callosum, red mesh the CA1 field, blue mesh the CA2 field, green mesh the CA3 field and yellow the Dentate Gyrus. The box mesh represents the mean position of the SRMN voxel used for the experiment. ***b***, An individual metabolic profile acquired from the right dorsal hippocampus, its LCModel fit (red dotted line) and the contributions from our metabolites or resonances-of-interest. No filtering was applied. ***c***, Three coronal slices representing the right dorsal hippocampus ROI, overlaid over the average of an EPI scan.

group averages are presented whenever possible. Of the considered dataset, four additional animals were excluded from the association between neurotransmitter ratios and FC data because of movement artifacts leading to low rs-fMRI data quality, resulting in 32 animals (20 CUS and 12 Control). By default no correction for multiple comparisons is presented and a stricter significance threshold of $p < 0.01$ was used. However, emphasis was placed on results surviving correction for the familywise error rate (FWER), correcting for the number of connections. Visualization of the altered connections was done using BrainNet Viewer (Xia et al., 2013; https://www.nitrc.org/projects/bnv; RRID:SCR_009446).

Hormone and behavioral assessment. These tests were performed before the MR scanning session. Anxiety-like behavior was tested in the elevated plus maze (EPM), as described by Pego et al. (2008). Testing, performed during the light phase of the day after the CUS protocol was completed, involved measuring the time spent in the open arms (OA) of the maze. On the following day, blood was collected from each rat by tail venipuncture at 08:00 A.M., before MRI scanning session. Centrifugation at 13,000 rpm during 15 min was used to separate the sera which was then kept at −80°C. Corticosterone (Cort) levels in the serum were assessed by ELISA (Enzo Life Sciences).

MR data acquisition. MRI scanning was performed on a preclinical BioSpec 11.7T scanner (Bruker) running on Paravision 6.0 (RRID: SCR_001964). A 72 mm diameter volume coil was used for transmission and a 4-channel phased array surface coil was used for reception. Before scanning, animals were anesthetized using 4–5% isoflurane in a 1:1 mixture of air and oxygen before being placed on a MR-compatible mechanical cradle; after fixing with bite and ear bars the concentration of isoflurane was reduced to 1–2% to maintain breathing at ~70/min. Throughout, body temperature was maintained at 37–38°C using a circulating hot water system. The scanning session included the acquisition of a three-shot SE-EPI sequence (TE/TR = 17.5/2000 ms, 450 repetitions, slice thickness of 750 μm, inter-slice gap of 0.25 mm in plane resolution of $375 \times 375\ \mu m^2$, FoV of $24 \times 24 \times 19.75\ mm^3$ covering the cerebrum but not the cerebellum nor the olfactory bulb) and a localized spectrum with the LASER (Garwood and DelaBarre, 2001) sequence (TE/TR = 25/3500 ms, 128 averages) from a 18 μl voxel positioned at the level of the right dorsal hippocampus. B_0-shimming was performed using the MAPSHIM Bruker routine leading to typical water linewidths of 11–13 Hz. Water suppression was achieved using VAPOR (Tkáč et al., 1999). A breathing wave trigger was used to reduce breathing movement artifacts. EPI data were reconstructed using an in-house developed MATLAB script.

MR data processing. Spectra were analyzed using LCModel 6.3 (Provencher, 1993; RRID:SCR_014455) and a simulated basis set. Twenty metabolites were considered and the macromolecule baseline was parameterized as described previously (Lopez-Kolkovsky et al., 2016). Metabolite concentrations were derived using total creatine (tCr = 8 mmol/L) as an internal reference of concentration. Based on the literature, eight metabolites or ratios-of-interest were considered in our statistical analysis: GABA and Glu, with their ratios to Gln ratios serving as an index of GABA and Glu metabolism, as well as myo-inositol (Ins), taurine (Tau), NAA (N-Acetylaspartic acid), total choline (tCho) and the group of macromolecular resonances visible between 0.9 and 1.9 ppm (MM1). The positioning of the voxel and a representative spectrum is depicted in Figure 1, *a* and *b*.

Processing of fMRI EPI data was done using FMRIB Software Library (FSL, https://fsl.fmrib.ox.ac.uk/fsl; RRID:SCR_002823). Preprocessing steps included slice timing and motion correction, motion scrubbing, and outlier detection, extraction of the skull from the brain, confound

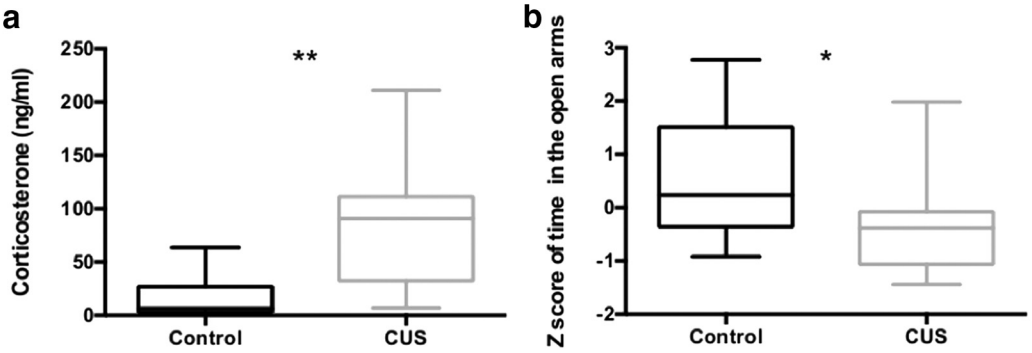

Figure 2. Comparison between control and CUS animals with: (***a***) corticosterone levels increased in the CUS animals (**$p < 10^{-4}$); (***b***), reduced time spent in the open arms for CUS animals (*$p = 0.008$). Boxes represent the 25–75th percentiles and whiskers range from the minimum to maximum values.

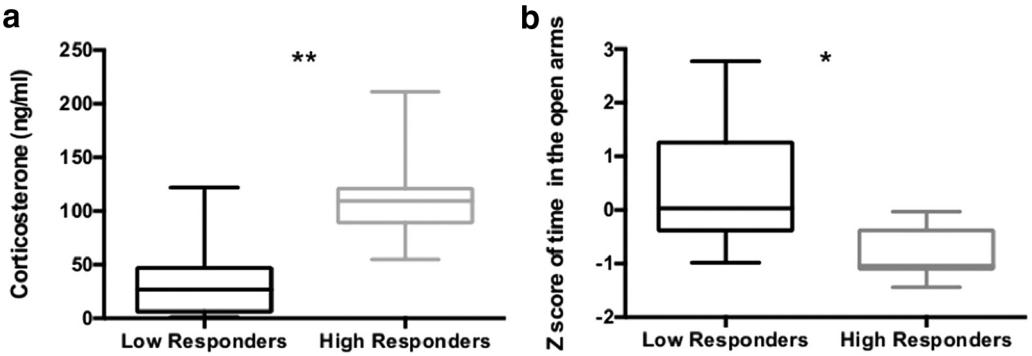

Figure 3. Comparison between Low- and High-responders to stress with: (***a***) corticosterone levels increased in the High-responder animals (**$p < 10^{-4}$); (***b***) reduced time spent in the OA for High-responder animals (*$p < 10^{-4}$). Boxes represent the 25–75th percentiles and whiskers range from the minimum to maximum values.

signal regression (excluding motion parameters, outliers, and average global signal), nonlinear registration to the in-house developed SIGMA template, spatial smoothing with a FWHM kernel of 8 mm, bandpass filtering between 0.005 and 0.1 Hz and artifact cleanup using single subject ICA (Kelly et al., 2010). Subjects with movement exceeding 0.975 mm were excluded from the analysis because of excessive motion.

The in-house developed SIGMA functional atlas, which divides the brain into 58 regions-of-interest (ROIs), built using a group ICA (Beckmann et al., 2005) and RAICAR (Yang et al., 2008) for component validation, was used to analyze the functional data. The signal from each ROI was extracted for each subject and the correlation between each ROI and the right dorsal hippocampus calculated and normalized using the fisher-*z* transformation to yield a measure of FC from the right dorsal hippocampus to the rest of the brain. The seed ROI and a sample of the functional data can be seen in Figure 1*c*.

Clustering. Animals were clustered into "high-responding" (high Cort, low OA time) and "low-responding" (low Cort, high OA time) groups, i.e., according to their basal Cort levels and time spent in the OA of the EPM. As described by Magalhães et al. (2018), a *k*-means clustering algorithm with two cluster centers was applied to the normalized biochemical and behavioral data. The rs-fMRI and MRS data were subsequently analyzed as a function of the degree of each individual animal's resistance or susceptibility to stress.

Results

Response to stress

The effectiveness of the CUS paradigm was confirmed by comparing serum Cort levels and time spent in the OA of the EPM. Serum Cort levels were increased in CUS-exposed rats versus control animals (t value $= 5.6$, df $= 30.7$, $p < 10^{-4}$, with Hedge's $g = 1.53$; Fig. 2*a*); CUS-treated rats spent less time in the OA of the EPM, suggesting their increased anxious-like behavior ($t = -2.8$, df $= 34$, $p = 0.008$, $g = 0.97$; Fig. 2*b*).

Using a *k*-means clustering algorithm, animals were divided into two clusters (Magalhães et al., 2018); this procedure produced clusters consisting of 10 animals each. Our previous observations were confirmed, with the High-responder cluster presenting reduced levels of Cort ($t_{(34)} = 6.9$, $p < 10^{-4}$, $g = 2.40$, independent two-sample t test; Fig. 3*a*) and increased time spent in the OA of the EPM ($t_{(34)} = -4.8$, $p < 10^{-4}$, $g = 1.30$, by independent two-sample t test; Fig. 3*b*) compared with the High-responders.

Neurometabolic changes with stress

Comparison of neurometabolite concentrations between control and CUS animals revealed that stress only caused a significant change in the GABA–Gln ratio (Table 1*a*). On the other hand, the High- and Low-responders showed significant differences in the concentrations of MM1 (survives FWER correction) and in the GABA–Gln and Glu–Gln ratios (Table 1*b*). Average spectra for both groups are depicted in Figure 4.

Testing for possible correlations between the significant neurometabolic changes (above) and Cort levels across all animals revealed significant positive associations for GABA/Gln ($\rho_{(34)} = 0.43$, $p = 0.008$; Fig. 5*a*) and Glu/Gln ($\rho_{(34)} = 0.36$, $p = 0.029$; Fig. 5*b*), and a negative association for MM1 ($\rho_{(34)} = -0.43$, $p = 0.009$, Fig. 5*c*). Examination of these correlations within each subgroup revealed stronger effects for GABA/Gln in the High-responders and smaller on low and control ($\rho_{\text{Ctrl-LowResp}} = 0.09$, $\rho_{\text{CUS-LowResp}} = 0.18$, and $\rho_{\text{CUS-HighResp}} = 0.35$). For Glu/Gln ($\rho_{\text{Ctrl-LowResp}} = 0.17$, $\rho_{\text{CUS-LowResp}} = 0.36$, and $\rho_{\text{CUS-HighResp}} = 0.14$) the association was stronger for the CUS Low-responders. In the case of MM1 effects, the correlations were negative and were stronger in Low-responders ($\rho_{\text{Ctrl-LowResp}} = 0.12$, $\rho_{\text{CUS-LowResp}} =$

Table 1. Differences in metabolite concentrations in the right dorsal hippocampus between: (*a*) Control and CUS animals; (*b*) the clusters of Low- and High-responders

	(*a*) Control vs CUS					(*b*) Low- vs High-responders				
	t	*p*	Mean Ctrl	Mean CUS	*g*	*t*	*p*	Mean Low	Mean High	*g*
GABA	−2	0.06	2.32	2.68	0.68	−1.24	0.22	2.47	2.71	0.43
GABA/Gln	**−2.1**	**0.04**	**0.71**	**0.90**	**0.71**	**−2.11**	**0.04**	**0.77**	**0.95**	**0.73**
Gln	0.47	0.64	3.31	3.19	0.16	1.51	0.14	3.36	2.98	0.52
Glu	0.58	0.56	9.57	9.23	0.19	−1.43	0.16	9.08	9.91	0.49
Glu/Gln	−0.59	0.56	2.94	3.13	0.20	**−2.05**	**0.05**	**2.87**	**3.46**	**0.71**
Ins	0.41	0.68	8.11	8.01	0.14	1.48	0.15	8.17	7.82	0.51
MM1	1.13	0.27	22.41	21.51	0.38	**3.05**	**0.004**	**22.59**	**20.12**	**1.06**
NAA	1.90	0.06	10.08	9.73	0.64	0.67	0.51	9.90	9.77	0.23
Tau	0.17	0.86	6.41	6.31	0.06	−1.39	0.17	6.09	6.86	0.48
tCho	−0.17	0.86	1.08	1.09	0.06	−0.27	0.79	1.08	1.09	0.09

Here presented is the t statistic (*t*), the test significance (*p*), mean values for each group and a measure of effect sizes (Hedge's *g*).

-0.36 and $\rho_{\text{CUS-HighResp}} = -0.19$). The individual fits are shown in Figure 5.

No significant associations were found between any of the metabolic changes and the time spent in the OA of the EPM.

Correlation between neurotransmitter levels and FC of the hippocampus

First, we tested the existence of differences in the FC of the right dorsal hippocampus between (1) Controls to CUS animals and (2) response clusters. Several effects were found in the first comparison (for statistics, see Table 2*a*), although none survives the full correction for multiple comparisons. For a threshold of $p < 0.01$, associations were found with the right primary cortex (Node 1) and the prelimbic cortex (Node 8). No effects surviving any threshold were found for the second comparison (Table 2*b*)

Next, we tested whether stress exposure impacted on the correlation between GABA–Gln ratio in the right dorsal hippocampus and its FC. For this, the interaction of the metabolite's ratio with the group membership was calculated as the product of the two. The interaction was used as variable-of-interest and the FC of each connection as the dependent variable. No associations survived either correction for multiple comparisons or a less-stringent threshold of $p < 0.01$. Weaker associations ($p < 0.05$) were found for the right posterior thalamic nucleus (Node 26), superior colliculus (Node 32), right entorhinal cortex (Node 41), and the right accumbens (Node 57).

Subsequently, we tested whether the correlation between GABA–Gln and Glu–Gln ratios in the right dorsal hippocampus and its FC were dependent on the response to stress in the exposed animals by examining the interaction with the response clusters. The approach described for the interaction with the group was again applied. Detailed results of this analysis are listed in Table 2, *c* and *d*, and shown in Figure 6, *a* and *b*. Briefly, significant associations were found between GABA/Gln and the clustering response to stress in the connection to the piriform cortex (Node 3: $t_{(30)} = 3.71$, $p = 0.002$, independent two-sample *t* test); the left thalamus (Node 18: $t_{(30)} = 3.98$, $p = 0.001$, independent two-sample *t* test, survived FWER correction); and the right amygdala (Node 34: $t_{(30)} = 3.01$, $p = 0.008$, independent two-sample *t* test). Notably among the other associations, albeit with lower levels of significance were those in connections to the nucleus accumbens, the striatum and the raphe nucleus. An interaction between the Glu–Gln ratio and the clustered response to stress was also associated with FC of the hippocampus (Fig. 6*d*,*e*). Strong associations were found in connections with the piriform cortex (Node 3: $t_{(30)} = 3.17$, $p = 0.006$, independent two-sample *t* test) and the left thalamus (Node 18: $t_{(30)} = 2.94$, $p = 0.009$, independent two-sample *t* test). Other associations, with lower significance, are presented in Table 2, among which is the right amygdala.

Last, these increases in the GABA–Gln and Glu–Gln ratios were associated with an average increase in FC in High-responders (Fig. 6*c*) and a decrease in Low-responders (Fig. 6*c*,*f*).

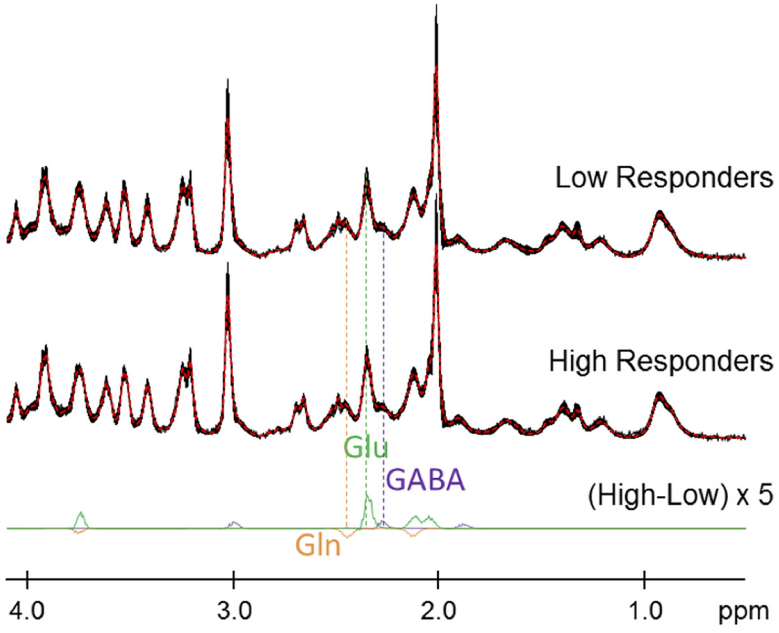

Figure 4. Average spectra for the Low- and High- responders (mean ± SD, black), corresponding LCModel fit (red dotted line) and average glutamate, glutamine, and GABA changes between both clusters.

Discussion

The present study used *in vivo* neuroimaging tools to reveal how chronic stress affects the metabolism of two key neurotransmitters (Glu and GABA) in the rat dorsal hippocampus; further it examined how these changes correlate with behavioral and endocrine biomarkers of stress s susceptibility in individual animals and FC patterns. We focused on the hippocampus because its structure (Sousa et al., 2000; McEwen, 2002) and function are

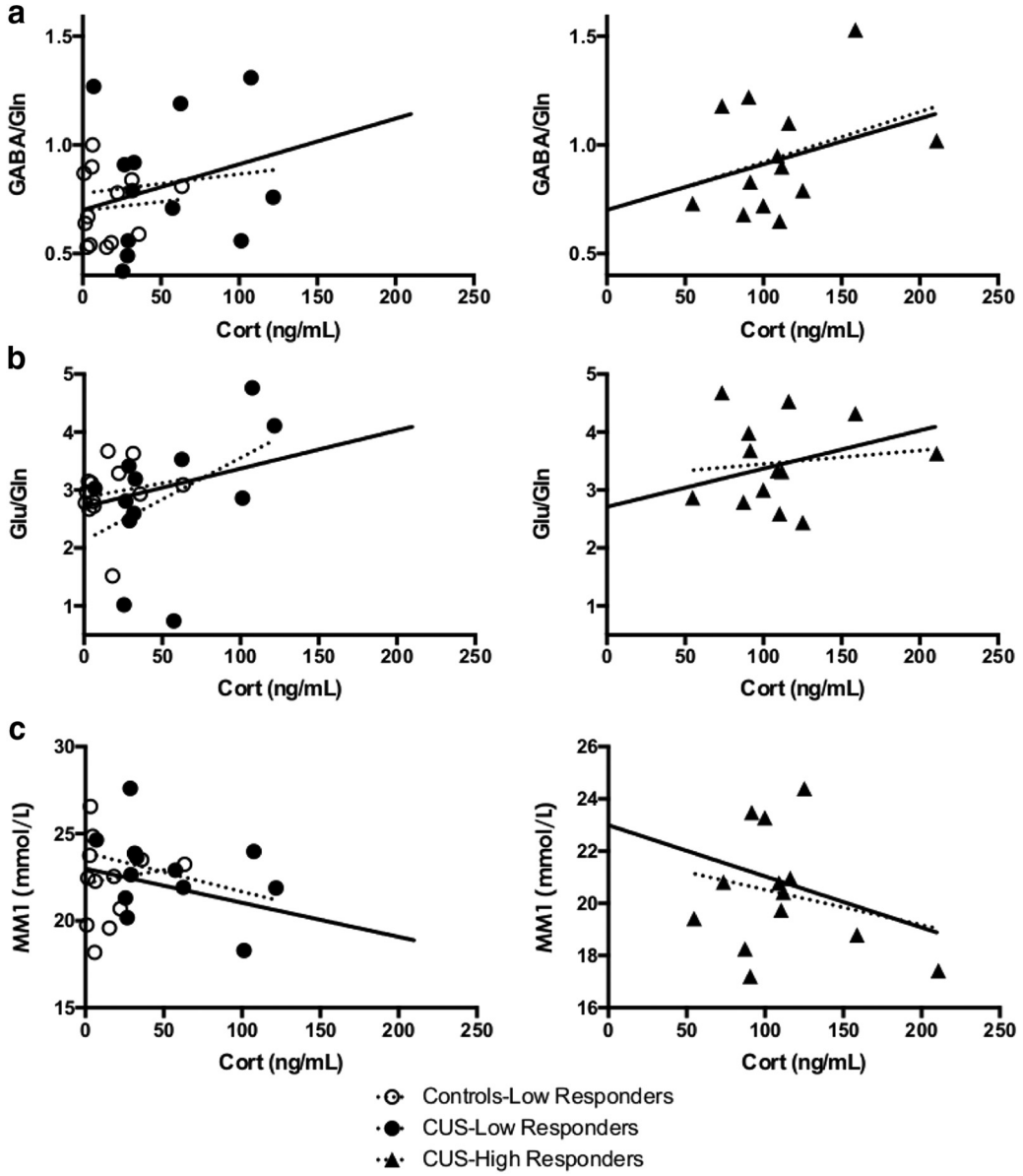

Figure 5. Associations between corticosterone levels and the metabolites found to be significantly different between clusters of response to stress: (***a***) GABA/Gln: $\rho = 0.43$, $p = 0.008$, df = 36; (***b***) Glu/Gln: $\rho = 0.36$, $p = 0.029$, df = 36; or (***c***) MM1: $\rho = -0.43$, $p = 0.009$, df = 36. Left, Low-responders; right, High-responders to stress. Compact lines represent the overall described association, whereas the individual dotted lines represent the different groups or clusters.

highly sensitive to stress (Luine et al., 1994; Conrad et al., 1996; Kim and Diamond, 2002).

Exposure to a CUS paradigm was accompanied by a rise in GABA concentrations in the dorsal hippocampus, indicating accumulation of the neurotransmitter, most likely in the intracellular compartment. Furthermore, levels of NAA in this area presented a decreasing trend, suggesting a compromise of neuronal integrity.

The response to stress is known to be heterogeneous, with some individuals being more susceptible to the impact of stress upon brain and behavior. After clustering animals as High- and Low-responders, based on their hormonal (corticosterone) and behavioral (anxiety-like behavior) responses, we sought neurometabolic signatures of resistance and susceptibility to stress. While concentrations of NAA, GABA, and Glu did not differ between High- and Low-responders, the ratios of GABA–Gln and Glu–Gln were higher in stress-susceptible animals. However, these results should be regarded with caution because the effect sizes were modest and did not survive correction for multiple comparisons. Nonetheless, the observed disruptions of GABAergic and glutamatergic metabolisms are consistent with the literature. Some authors reported that stress increased glutamate/tCr levels in the ventral hippocampus (Delgado y Palacios et al., 2011), increased GABA levels in the dorsal hippocampus (de Groote and Linthorst, 2007) and anterior cingulate (Perrine et al., 2014); on the other hand, others recorded stress-induced decreases in the concentrations of Glu and GABA in these brain regions (Hemanth Kumar et al., 2012; Shao et al., 2015).

Furthermore we found decreased levels of MM1 in High-responders (strong effect size). The MM1 signal was detected by resonances that mostly correspond to those produced by methylene and methyl groups in semi-mobile macromolecules (proteins and lipids; Behar et al., 1994). Reduction of this signal likely reflects activation of cellular stress, inhibition of

Table 2. Associations between the FC of the right dorsal hippocampus and every ROI in the SIGMA atlas

		(*a*) Control vs CUS		(*b*) Low- vs High-responders		(*c*) GABA/Gln		(*d*) Glu/Gln	
	No.	*p*	*t*	*p*	*t*	*p*	*t*	*p*	*t*
Right primary somatosensory	1	**0.006**	**2.93**	0.819	−0.23	0.376	0.91	0.497	0.7
Right cingulate cortex	2	0.657	0.45	0.441	0.79	0.569	0.58	0.302	1.07
Right piriform cortex	3	0.131	1.55	0.060	2.01	**0.002**	**3.71**	**0.006**	**3.17**
Right primary somatosensory cortex (BE)	4	0.366	0.92	0.552	−0.61	0.181	1.4	0.152	1.5
Left posterior lateral striatum	5	0.255	1.16	0.637	−0.48	0.073	1.92	0.179	1.4
Cingulate cortex 2	6	0.051	2.03	0.983	0.02	0.103	1.73	0.368	0.93
Cingulate cortex 3	7	0.887	0.14	0.851	0.19	0.710	0.38	0.528	0.65
Prelimbic cortex	8	**0.004**	**3.10**	0.419	−0.83	0.206	1.32	0.466	0.75
Right temporal association cortex	9	0.577	0.56	0.116	−1.65	0.410	0.85	0.326	1.01
Cingulate cortex 1	10	0.173	1.40	0.585	−0.56	0.955	−0.07	0.973	−0.03
Left primary somatosensory	11	0.055	1.99	0.569	−0.58	0.086	1.83	0.296	1.08
Left primary somatosensory cortex (BE)	12	0.121	1.60	0.670	−0.43	0.161	1.47	0.185	1.39
Left pontine reticular/subcoeruleus	13	0.863	0.17	0.950	0.06	0.079	1.88	0.538	0.63
Right striatum	14	0.284	1.09	0.324	−1.01	**0.020**	**2.58**	0.275	1.13
Retrosplenial cortex	15	0.577	0.56	0.310	−1.05	0.956	−0.06	0.319	1.03
Left dorsal medial striatu,	16	0.178	1.38	0.546	−0.62	0.408	0.85	0.277	1.13
Left CA1 (transition dorsal ventral)	17	0.714	−0.37	0.576	−0.57	0.361	0.94	0.348	0.97
Left ventrolateral thalamic	18	0.512	0.66	0.833	0.21	**0.001**	**3.98**	**0.010**	**2.94**
Left CA3 hippocampus	19	0.646	0.46	0.607	−0.52	0.171	1.43	0.090	1.81
Left insular cortex	20	0.200	1.31	0.438	−0.79	0.165	1.46	0.107	1.71
Raphe (pallidum/magnun) nuclei	21	0.670	−0.43	0.579	0.56	**0.030**	**2.39**	**0.013**	**2.78**
Pontine nuclei	22	0.408	−0.84	0.695	0.40	0.084	1.85	0.384	0.89
Retrosplenial cortex	23	0.583	0.55	0.271	−1.14	0.443	0.79	0.141	1.55
Right Postsubiculum/retrosplenial granular cortex zone A	24	0.528	0.64	0.523	0.65	0.881	−0.15	0.864	0.17
Right Subcoeruleum/pontine reticular nu	25	0.229	−1.23	0.411	0.84	**0.022**	**2.53**	0.128	1.61
Right posterior thalamic nucleus	26	0.425	−0.81	0.881	0.15	0.095	1.78	0.076	1.9
Left amygdalar nuclei (Ce)	27	0.417	0.82	0.378	0.90	**0.022**	**2.53**	**0.050**	**2.12**
Right medial mammillary nucleus	28	0.074	−1.85	0.885	0.15	**0.021**	**2.56**	0.607	0.52
Left accumbens	29	0.452	0.76	0.927	−0.09	0.174	1.42	0.357	0.95
Right lateral accumbens shell	30	0.082	1.80	0.489	0.71	**0.019**	**2.6**	**0.011**	**2.89**
Right insular cortex	31	**0.030**	**2.27**	0.492	−0.70	0.168	1.44	0.053	2.09
Superior colliculus	32	0.369	0.91	0.390	0.88	0.431	0.81	0.063	2
Right subiculum	33	0.563	−0.58	0.059	2.01	0.101	1.74	0.185	1.38
Right amygdala (central, BLA, nuclei)	34	0.167	1.42	0.108	−1.69	**0.008**	**3.01**	**0.049**	**2.14**
Right (medial) habenular nuclei	35	0.727	−0.35	0.888	0.14	0.500	0.69	0.451	0.77
Right Raphe/median(paramedian) pontine reticular nucleus	36	0.435	0.79	0.938	−0.08	**0.029**	**2.4**	0.158	1.48
Left interpeduncular nucleus	37	0.926	0.09	0.393	0.88	0.446	0.78	0.993	−0.01
Hypothalamus	38	0.867	0.17	0.529	0.64	0.147	1.52	0.373	0.92
Right Septal nucleus (triangular)	39	0.061	1.95	0.277	1.12	0.423	0.82	0.478	0.73
Left dorsal dentate gyrus of the hippocampal formation	40	0.939	−0.08	0.453	−0.77	0.507	0.68	0.271	1.14
Right intermedial entorhinal cortex	41	0.766	0.30	0.750	0.32	0.283	1.11	0.349	0.97
Right primary/secondary visual cortex	43	0.351	0.95	0.478	−0.72	0.492	0.7	0.338	0.99
Left subiculum (parasubiculum)	44	0.747	−0.33	0.759	0.31	0.243	−1.21	0.624	−0.5
Left CA1 (ventral)	45	0.646	0.46	0.610	−0.52	0.549	0.61	0.591	0.55
Retrosplenial granular cortex c	46	0.156	1.45	0.536	−0.63	0.876	0.16	0.217	1.29
Right ventral tegmental nucleus	47	0.924	0.10	0.476	0.73	0.134	1.58	0.477	0.73
Right external cortex inferior colliculus	48	0.257	−1.16	0.367	0.93	0.473	0.73	0.414	0.84
Left parasubiculum	49	0.136	−1.53	0.400	−0.86	0.876	−0.16	0.904	−0.12
Dorsal lateral PAG	50	0.664	0.44	0.221	1.27	0.088	1.81	0.173	1.43
Left medial geniculate nucleus	51	0.895	0.13	0.792	0.27	0.128	1.61	0.214	1.29
Right inferior colliculus	52	0.287	−1.08	0.548	0.61	0.366	0.93	0.543	0.62
Retrosplenial cortex	53	**0.012**	**2.68**	0.955	0.06	0.524	−0.65	0.725	0.36
Left piriform cortex	54	0.189	1.34	0.240	1.22	0.558	0.6	0.234	1.24
Left striatum	55	0.692	0.40	0.688	−0.41	**0.024**	**2.49**	0.074	1.91
Left retrosplenial granular cortex a	56	0.226	1.24	0.706	0.38	0.967	0.04	0.843	0.2
Right accumbens	57	0.118	1.61	0.428	0.81	0.944	0.07	0.849	0.19
Left primary visual cortex	58	0.769	−0.30	0.277	−1.12	0.726	0.356	0.530	0.64

(*a*) Comparison between Control and CUS animals; (*b*) comparison between Low- and High-responders to stress; (*c*) GABA/Gln-Cluster interaction with FC; (*d*) Glu/Gln-Cluster interaction with FC. Here presented is the t statistic (*t*) and the test significance (*p*; with higher significances highlighted).

cell proliferation and/or alterations in the brain lipidome (Oliveira et al., 2016), specifically, of ceramide (Gulbins et al., 2013; Oliveira et al., 2016). The ceramide pathway, recently linked to adult hippocampal neurogenesis (Gulbins et al., 2013, 2016), may therefore play a role in the development of stress-related diseases, and help explain the bifurcation in the responses to stress.

It is pertinent to note that inconsistencies between MRS-based findings may be attributed to technical issues. For example, (1) the spectra reported by Hong et al. (2009) were acquired using a TE of 144 ms although macromolecules and J-coupled metabolites (e.g., GABA, Glu) have very short-lived signals; (2) even though Hemanth Kumar et al. (2012) used a spectroscopic voxel (24 μl) comparable to that used by us, their spectral decomposi-

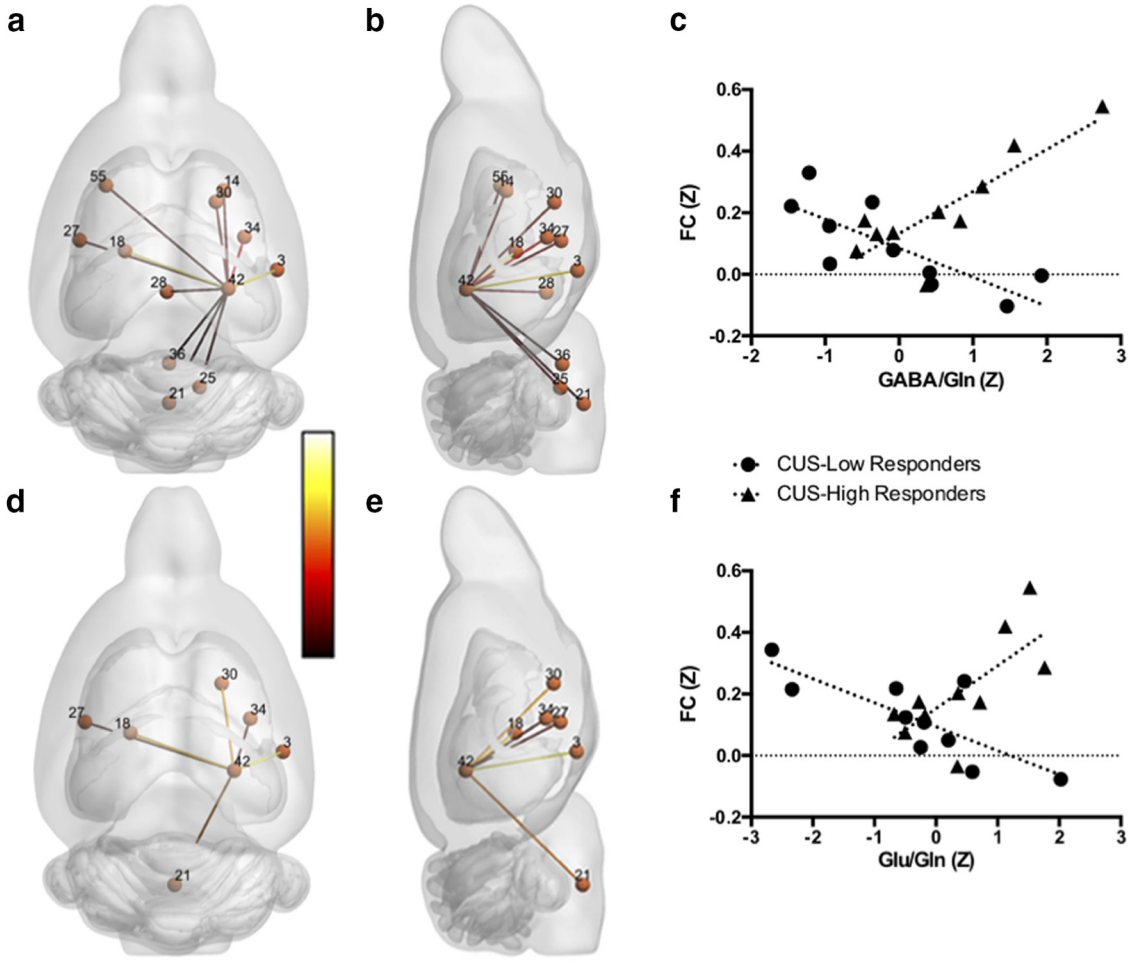

Figure 6. Significant associations between the interaction of GABA and glutamatergic metabolism with response cluster and functional connections of the right dorsal hippocampus: (***a***) axial and (***b***) sagittal views of the connections with significant associations for GABA/Gln × Cluster; (***c***) plot of the association between the average FC of the significant connections from ***a*** and ***b*** for each subject and the GABA–Gln ratio; (***d***) axial and (***e***) sagittal views of the connections with significant interactions for Glu/Gln; (***f***) plot of the association between the average functional connectivity of the significant connections from ***d*** and ***e*** for each subject and the Glu/Gln ratio, where we plot the average FC of the significant connections against the metabolite ratios for each cluster of animals. We show all connections where $p < 0.05$. Connections color-coded in "hot" color-map.

tion exhibited a free-moving macromolecule baseline that could contribute to substantial quantification errors (Xin and Tkáč, 2017); and (3) Shao et al. (2015) appear to have used an inappropriate free-moving macromolecule baseline.

By considering GABA–glutamine and glutamate–glutamine ratios as proxy measures of metabolism in hippocampal neurons, we observed associations with serum corticosterone levels but not with changes in anxious-like behavior, a stress-related adaptation. The reasons for this apparent discrepancy are twofold. First, because corticosterone and the measured metabolites directly reflect tightly-regulated brain biochemistry, interactions between them are more likely to be detected than interactions between neurotransmitter-hormone levels and behavior. Second, behavioral measures such as anxiety-like behavior are a summation of multiple inputs that are influenced by many factors that are, arguably, less easily related to specific changes in neurotransmitter levels. As discussed below, this view is supported by previous reports that describe how high levels of corticosterone directly impact on neurotransmitter and receptor expression.

Increases in glutamate turnover in the hippocampus have been previously described in the context of the stressed brain (Lowy et al., 1995; Venero and Borrell, 1999; Delgado y Palacios et al., 2011; Popoli et al., 2011). Increased extracellular glutamate levels have been associated with glucocorticoid-induced (Stein-Behrens et al., 1994; Venero and Borrell, 1999) neuronal atrophy or reduced neurogenesis (Cameron et al., 1995; Sapolsky, 2000). Because glucocorticoids reduce glutamate reuptake (Olivenza et al., 2000; Yang et al., 2005) and increase glutamatergic neuron excitability (Musazzi et al., 2011), we interpret our observations as being suggestive of stress-elicited increases of *de novo* synthesis of glutamate with parallel reductions in the rate of glutamate-glutamine recycling. However, given that glutamate is a precursor of GABA, it is conceivable that the changes observed are mainly because of alterations in inhibitory pathways; the overlap of FC nodes and connections observed makes this notion plausible.

Notably, the increased FC in High-responders, linked to the metabolic changes therein, is likely to be functionally important. Increased synchronization of large populations of neurons and subsequently, increased FC between distant brain areas arise by filtering out small local oscillations that favor the emergence of gamma fluctuations corresponding to global states of synchronicity (Fingelkurts et al., 2004; Pathak et al., 2016); importantly, these are linked to GABAergic inhibition, as supported by the present data. On the other hand, decreased FC, accompanied by higher GABA and glutamatergic metabolism in Low-responders,

likely reflects a balance between excitation and inhibition that endures stressful insults.

Reinforced connections between the hippocampus and amygdala have been previously described (Pitkänen et al., 2000), as have their interactions in the context of stress-associated modulation of memory formation and learning (Akirav and Richter-Levin, 1999; Richter-Levin and Akirav, 2000; Kim et al., 2001; Roozendaal et al., 2009). The thalamus plays a key role in the relay of information between different parts of the limbic system (Su and Bentivoglio, 1990). In particular the anterior-dorsal nuclei, with which our region of interest partially overlaps, are known to project to the hippocampus (Wyss et al., 1979; Amaral and Cowan, 1980; Shah et al., 2012; Jankowski et al., 2013) and to be involved in memory formation and retrieval (Harding et al., 2000; Stein et al., 2000; Aggleton et al., 2010; Dillingham et al., 2015). The piriform cortex is not typically studied in stress. Mainly associated with odor processing (Staubli et al., 1987; Haberly, 2001), this area, and in particular its posterior components (Litaudon et al., 2003) has been shown to have multiple functions including a role in integration of information (Calu et al., 2007); in fact, it plays a similar role to the thalamus with which it shares strong connections (Ray and Price, 1992). In the context of stress, the piriform cortex and its association with the amygdala are thought to play an important role in the integration of predatory scent information and fear conditioning (Kondoh et al., 2016), a process which may be key in determining response to stress. The piriform cortex, thalamus, and amygdala show commonalities in their relationship with the hippocampus with respect to the integration and retrieval of fear-related memories. From a higher-order system perspective, a striking feature of these results is that they all involve sub-elements of the limbic system. This becomes more evident by considering the participation of the striatum, the raphé nucleus and the accumbens, also found to display altered connectivity in response to stress. The limbic system is a key mediator of the stress response (Morgane et al., 2005), through its close association with the HPA axis and the raphé and the interaction between the serotonergic system, and GABAergic pathways (Jacobs and Azmitia, 1992).

Regarding the overall effect of CUS on FC, our results point to interdependency between the alterations in FC and the neurotransmitter ratios. As the comparison of the response is not enough to explain the hippocampal related changes in CUS phenotype (Table 2*b*), it stands to reason that other variables may be necessary to explain them. Furthermore, as we see in Figure 5, the changes in the neurotransmitter ratios are likely related to corticosterone levels, suggesting that this increase may push the system past a critical point, altering the nature of excitatory and inhibitory circuits of the hippocampus, leading to increased synchronicity with different regions.

A few limitations of this work should be mentioned. It remains unclear whether the neurotransmitter alterations drive the changes in connectivity or vice versa, or whether they are independently driven by a common factor (e.g., perhaps corticosterone) or the direction of changes in connectivity. The MRI and MRS acquisitions were done under light anesthesia, which could potentially dampen signal detection and reduce the range of functional and neurotransmitter dynamics. The classification of the response to stress considered only two dimensions of the response, making it critical to explore other dimensions in future studies, consider more complex classifications and even a spectrum of responses.

In conclusion, this study demonstrates that chronic stress alters neurotransmitter metabolism in the dorsal hippocampus and relates these changes to alterations in FC of the brain. The present observations are consistent with literature documenting the remodeling of the hippocampus and related structures by chronic stress.

References

Abdallah CG, Jiang L, De Feyter HM, Fasula M, Krystal JH, Rothman DL, Mason GF, Sanacora G (2014) Glutamate metabolism in major depressive disorder. Am J Psychiatry 171:1320–1327.

Abdallah CG, De Feyter HM, Averill LA, Jiang L, Averill CL, Chowdhury GMI, Purohit P, de Graaf RA, Esterlis I, Juchem C, Pittman BP, Krystal JH, Rothman DL, Sanacora G, Mason GF (2018) The effects of ketamine on prefrontal glutamate neurotransmission in healthy and depressed subjects. Neuropsychopharmacology 43:2154–2160.

Aggleton JP, O'Mara SM, Vann SD, Wright NF, Tsanov M, Erichsen JT (2010) Hippocampal-anterior thalamic pathways for memory: uncovering a network of direct and indirect actions. Eur J Neurosci 31:2292–2307.

Akirav I, Richter-Levin G (1999) Biphasic modulation of hippocampal plasticity by behavioral stress and basolateral amygdala stimulation in the rat. J Neurosci 19:10530–10535.

Amaral DG, Cowan WM (1980) Subcortical afferents to the hippocampal formation in the monkey. J Comp Neurol 189:573–591.

Anacker C, Scholz J, O'Donnell KJ, Allemang-Grand R, Diorio J, Bagot RC, Nestler EJ, Hen R, Lerch JP, Meaney MJ (2016) Neuroanatomic differences associated with stress susceptibility and resilience. Biol Psychiatry 79:840–849.

Beckmann CF, DeLuca M, Devlin JT, Smith SM (2005) Investigations into resting-state connectivity using independent component analysis. Philos Trans R Soc Lond B Biol Sci 360:1001–1013.

Behar KL, Rothman DL, Spencer DD, Petroff OA (1994) Analysis of macromolecule resonances in 1H NMR spectra of human brain. Magn Reson Med 32:294–302.

Bondi CO, Rodriguez G, Gould GG, Frazer A, Morilak DA (2008) Chronic unpredictable stress induces a cognitive deficit and anxiety-like behavior in rats that is prevented by chronic antidepressant drug treatment. Neuropsychopharmacology 33:320–331.

Brown SM, Henning S, Wellman CL (2005) Mild, short-term stress alters dendritic morphology in rat medial prefrontal cortex. Cereb Cortex 15:1714–1722.

Calu DJ, Roesch MR, Stalnaker TA, Schoenbaum G (2007) Associative encoding in posterior piriform cortex during odor discrimination and reversal learning. Cereb Cortex 17:1342–1349.

Cameron HA, McEwen BS, Gould E (1995) Regulation of adult neurogenesis by excitatory input and NMDA receptor activation in the dentate gyrus. J Neurosci 15:4687–4692.

Cerqueira JJ, Mailliet F, Almeida OF, Jay TM, Sousa N (2007) The prefrontal cortex as a key target of the maladaptive response to stress. J Neurosci 27:2781–2787.

Chen X, Fan X, Hu Y, Zuo C, Whitfield-Gabrieli S, Holt D, Gong Q, Yang Y, Pizzagalli DA, Du F, Ongur D (2018) Regional GABA concentrations modulate inter-network resting-state functional connectivity. Cereb Cortex. Advance online publication. Retrieved July 25, 2018. doi:10.1093/cercor/bhy059.

Conrad CD, Galea LA, Kuroda Y, McEwen BS (1996) Chronic stress impairs rat spatial memory on the Y maze, and this effect is blocked by tianeptine treatment. Behav Neurosci 110:1321–1334.

Czéh B, Michaelis T, Watanabe T, Frahm J, de Biurrun G, van Kampen M, Bartolomucci A, Fuchs E (2001) Stress-induced changes in cerebral metabolites, hippocampal volume, and cell proliferation are prevented by antidepressant treatment with tianeptine. Proc Natl Acad Sci U S A 98:12796–12801.

de Groote L, Linthorst AC (2007) Exposure to novelty and forced swimming evoke stressor-dependent changes in extracellular GABA in the rat hippocampus. Neuroscience 148:794–805.

Delgado y Palacios R, Campo A, Henningsen K, Verhoye M, Poot D, Dijkstra J, Van Audekerke J, Benveniste H, Sijbers J, Wiborg O, Van der Linden A (2011) Magnetic resonance imaging and spectroscopy reveal differential hippocampal changes in anhedonic and resilient subtypes of the chronic mild stress rat model. Biol Psychiatry 70:449–457.

Dias-Ferreira E, Sousa JC, Melo I, Morgado P, Mesquita AR, Cerqueira JJ, Costa RM, Sousa N (2009) Chronic stress causes frontostriatal reorganization and affects decision-making. Science 325:621–625.

Dillingham CM, Erichsen JT, O'Mara SM, Aggleton JP, Vann SD (2015) Fornical and nonfornical projections from the rat hippocampal formation to the anterior thalamic nuclei. Hippocampus 25:977–992.

Doyère V, Burette F, Negro CR, Laroche S (1993) Long-term potentiation of hippocampal afferents and efferents to prefrontal cortex: implications for associative learning. Neuropsychologia 31:1031–1053.

Fingelkurts AA, Fingelkurts AA, Kivisaari R, Pekkonen E, Ilmoniemi RJ, Kähkönen S (2004) Enhancement of GABA-related signalling is associated with increase of functional connectivity in human cortex. Hum Brain Mapp 22:27–39.

Garwood M, DelaBarre L (2001) The return of the frequency sweep: designing adiabatic pulses for contemporary NMR. J Magn Reson 153:155–177.

Gray JD, Rubin TG, Kogan JF, Marrocco J, Weidmann J, Lindkvist S, Lee FS, Schmidt EF, McEwen BS (2018) Translational profiling of stress-induced neuroplasticity in the CA3 pyramidal neurons of BDNF Val66Met mice. Mol Psychiatry 23:904–913.

Grønli J, Fiske E, Murison R, Bjorvatn B, Sørensen E, Ursin R, Portas CM (2007) Extracellular levels of serotonin and GABA in the hippocampus after chronic mild stress in rats: a microdialysis study in an animal model of depression. Behav Brain Res 181:42–51.

Gulbins A, Grassmé H, Hoehn R, Wilker B, Soddemann M, Kohnen M, Edwards MJ, Kornhuber J, Gulbins E (2016) Regulation of neuronal stem cell proliferation in the hippocampus by endothelial ceramide. Cell Physiol Biochem 39:790–801.

Gulbins E, Palmada M, Reichel M, Lüth A, Böhmer C, Amato D, Müller CP, Tischbirek CH, Groemer TW, Tabatabai G, Becker KA, Tripal P, Staedtler S, Ackermann TF, van Brederode J, Alzheimer C, Weller M, Lang UE, Kleuser B, Grassmé H, et al. (2013) Acid sphingomyelinase-ceramide system mediates effects of antidepressant drugs. Nat Med 19:934–938.

Haag L, Quetscher C, Dharmadhikari S, Dydak U, Schmidt-Wilcke T, Beste C (2015) Interrelation of resting state functional connectivity, striatal GABA levels, and cognitive control processes. Hum Brain Mapp 36:4383–4393.

Haberly LB (2001) Parallel-distributed processing in olfactory cortex: new insights from morphological and physiological analysis of neuronal circuitry. Chem Senses 26:551–576.

Harding A, Halliday G, Caine D, Kril J (2000) Degeneration of anterior thalamic nuclei differentiates alcoholics with amnesia. Brain 123:141–154.

Hemanth Kumar BS, Mishra SK, Rana P, Singh S, Khushu S (2012) Neurodegenerative evidences during early onset of depression in CMS rats as detected by proton magnetic resonance spectroscopy at 7 T. Behav Brain Res 232:53–59.

Henckens MJ, van der Marel K, van der Toorn A, Pillai AG, Fernández G, Dijkhuizen RM, Joëls M (2015) Stress-induced alterations in large-scale functional networks of the rodent brain. Neuroimage 105:312–322.

Hong ST, Choi CB, Park C, Moon HY, Hong KS, Cheong C, Chae JH, Choe BY (2009) Specific hippocampal choline decrease in an animal model of depression. Br J Radiol 82:549–553.

Ip IB, Berrington A, Hess AT, Parker AJ, Emir UE, Bridge H (2017) Combined fMRI-MRS acquires simultaneous glutamate and BOLD-fMRI signals in the human brain. Neuroimage 155:113–119.

Jacobs BL, Azmitia EC (1992) Structure and function of the brain serotonin system. Physiol Rev 72:165–229.

Jacobson L, Sapolsky R (1991) The role of the hippocampus in feedback regulation of the hypothalamic-pituitary-adrenocortical axis. Endocr Rev 12:118–134.

Jankowski MM, Ronnqvist KC, Tsanov M, Vann SD, Wright NF, Erichsen JT, Aggleton JP, O'Mara SM (2013) The anterior thalamus provides a subcortical circuit supporting memory and spatial navigation. Front Syst Neurosci 7:45.

Jay TM, Rocher C, Hotte M, Naudon L, Gurden H, Spedding M (2004) Plasticity at hippocampal to prefrontal cortex synapses is impaired by loss of dopamine and stress: importance for psychiatric diseases. Neurotox Res 6:233–244.

Kelly RE Jr, Alexopoulos GS, Wang Z, Gunning FM, Murphy CF, Morimoto SS, Kanellopoulos D, Jia Z, Lim KO, Hoptman MJ (2010) Visual inspection of independent components: defining a procedure for artifact removal from fMRI data. J Neurosci Methods 189:233–245.

Kim JJ, Diamond DM (2002) The stressed hippocampus, synaptic plasticity and lost memories. Nat Rev Neurosci 3:453–462.

Kim JJ, Lee HJ, Han JS, Packard MG (2001) Amygdala is critical for stress-induced modulation of hippocampal long-term potentiation and learning. J Neurosci 21:5222–5228.

Knox D, Perrine SA, George SA, Galloway MP, Liberzon I (2010) Single prolonged stress decreases glutamate, glutamine, and creatine concentrations in the rat medial prefrontal cortex. Neurosci Lett 480:16–20.

Kondoh K, Lu Z, Ye X, Olson DP, Lowell BB, Buck LB (2016) A specific area of olfactory cortex involved in stress hormone responses to predator odours. Nature 532:103–106.

Litaudon P, Amat C, Bertrand B, Vigouroux M, Buonviso N (2003) Piriform cortex functional heterogeneity revealed by cellular responses to odours. Eur J Neurosci 17:2457–2461.

Llorente R, Villa P, Marco EM, Viveros MP (2012) Analyzing the effects of a single episode of neonatal maternal deprivation on metabolite profiles in rat brain: a proton nuclear magnetic resonance spectroscopy study. Neuroscience 201:12–19.

Lopez-Kolkovsky AL, Mériaux S, Boumezbeur F (2016) Metabolite and macromolecule T1 and T2 relaxation times in the rat brain in vivo at 17.2T. Magn Reson Med 75:503–514.

Lowy MT, Wittenberg L, Yamamoto BK (1995) Effect of acute stress on hippocampal glutamate levels and spectrin proteolysis in young and aged rats. J Neurochem 65:268–274.

Luine V, Villegas M, Martinez C, McEwen BS (1994) Repeated stress causes reversible impairments of spatial memory performance. Brain Res 639:167–170.

Magalhães R, Bourgin J, Boumezbeur F, Marques P, Bottlaender M, Poupon C, Djemaï B, Duchesnay E, Mériaux S, Sousa N, Jay TM, Cachia A (2017) White matter changes in microstructure associated with a maladaptive response to stress in rats. Transl Psychiatry 7:e1009.

Magalhães R, Barrière DA, Novais A, Marques F, Marques P, Cerqueira J, Sousa JC, Cachia A, Boumezbeur F, Bottlaender M, Jay TM, Mériaux S, Sousa N (2018) The dynamics of stress: a longitudinal MRI study of rat brain structure and connectome. Mol Psychiatry 23:1998–2006.

McEwen BS (2002) Sex, stress and the hippocampus: allostasis, allostatic load and the aging process. Neurobiol Aging 23:921–939.

Morgane PJ, Galler JR, Mokler DJ (2005) A review of systems and networks of the limbic forebrain/limbic midbrain. Prog Neurobiol 75:143–160.

Musazzi L, Racagni G, Popoli M (2011) Stress, glucocorticoids and glutamate release: effects of antidepressant drugs. Neurochem Int 59:138–149.

Nephew BC, Febo M, Huang W, Colon-Perez LM, Payne L, Poirier GL, Greene O, King JA (2018) Early life social stress and resting state functional connectivity in postpartum rat anterior cingulate circuits. J Affect Disord 229:213–223.

Oliveira TG, Chan RB, Bravo FV, Miranda A, Silva RR, Zhou B, Marques F, Pinto V, Cerqueira JJ, Di Paolo G, Sousa N (2016) The impact of chronic stress on the rat brain lipidome. Mol Psychiatry 21:80–88.

Olivenza R, Moro MA, Lizasoain I, Lorenzo P, Fernández AP, Rodrigo J, Boscá L, Leza JC (2000) Chronic stress induces the expression of inducible nitric oxide synthase in rat brain cortex. J Neurochem 74:785–791.

Pathak Y, Salami O, Baillet S, Li Z, Butson CR (2016) Longitudinal changes in depressive circuitry in response to neuromodulation therapy. Front Neural Circuits 10:50.

Pego JM, Morgado P, Pinto LG, Cerqueira JJ, Almeida OF, Sousa N (2008) Dissociation of the morphological correlates of stress-induced anxiety and fear. Eur J Neurosci 27:1503–1516.

Perrine SA, Ghoddoussi F, Michaels MS, Sheikh IS, McKelvey G, Galloway MP (2014) Ketamine reverses stress-induced depression-like behavior and increased GABA levels in the anterior cingulate: an 11.7 T 1H-MRS study in rats. Prog Neuropsychopharmacol Biol Psychiatry 51:9–15.

Pitkänen A, Pikkarainen M, Nurminen N, Ylinen A (2000) Reciprocal connections between the amygdala and the hippocampal formation, perirhinal cortex, and postrhinal cortex in rat: a review. Ann N Y Acad Sci 911:369–391.

Popoli M, Yan Z, McEwen BS, Sanacora G (2011) The stressed synapse: the impact of stress and glucocorticoids on glutamate transmission. Nat Rev Neurosci 13:22–37.

Provencher SW (1993) Estimation of metabolite concentrations from localized *in vivo* proton NMR spectra. Magn Reson Med 30:672–679.

Ray JP, Price JL (1992) The organization of the thalamocortical connections of the mediodorsal thalamic nucleus in the rat, related to the ventral forebrain-prefrontal cortex topography. J Comp Neurol 323:167–197.

Richter-Levin G, Akirav I (2000) Amygdala-hippocampus dynamic interaction in relation to memory. Mol Neurobiol 22:11–20.

Roozendaal B, McEwen BS, Chattarji S (2009) Stress, memory and the amygdala. Nat Rev Neurosci 10:423–433.

Sanacora G, Mason GF, Rothman DL, Krystal JH (2002) Increased occipital cortex GABA concentrations in depressed patients after therapy with selective serotonin reuptake inhibitors. Am J Psychiatry 159:663–665.

Sapolsky RM (2000) Glucocorticoids and hippocampal atrophy in neuropsychiatric disorders. Arch Gen Psychiatry 57:925–935.

Shah A, Jhawar SS, Goel A (2012) Analysis of the anatomy of the papez circuit and adjoining limbic system by fiber dissection techniques. J Clinl Neurosci 19:289–298.

Shao Y, Yan G, Xuan Y, Peng H, Huang QJ, Wu R, Xu H (2015) Chronic social isolation decreases glutamate and glutamine levels and induces oxidative stress in the rat hippocampus. Behav Brain Res 282:201–208.

Sousa N (2016) The dynamics of the stress neuromatrix. Mol Psychiatry 21:302–312.

Sousa N, Lukoyanov NV, Madeira MD, Almeida OF, Paula-Barbosa MM (2000) Reorganization of the morphology of hippocampal neurites and synapses after stress-induced damage correlates with behavioral improvement. Neuroscience 97:253–266.

Staubli U, Schottler F, Nejat-Bina D (1987) Role of dorsomedial thalamic nucleus and piriform cortex in processing olfactory information. Behav Brain Res 25:117–129.

Stein T, Moritz C, Quigley M, Cordes D, Haughton V, Meyerand E (2000) Functional connectivity in the thalamus and hippocampus studied with functional MR imaging. Am J Neuroradiol 21:1397–1401.

Stein-Behrens BA, Lin WJ, Sapolsky RM (1994) Physiological elevations of glucocorticoids potentiate glutamate accumulation in the hippocampus. J Neurochem 63:596–602.

Su HS, Bentivoglio M (1990) Thalamic midline cell populations projecting to the nucleus accumbens, amygdala, and hippocampus in the rat. J Comp Neurol 297:582–593.

Tkáč I, Starčuk Z, Choi IY, Gruetter R (1999) In vivo 1H NMR spectroscopy of rat brain at 1 ms echo time. Magn Reson Med 41:649–656.

Venero C, Borrell J (1999) Rapid glucocorticoid effects on excitatory amino acid levels in the hippocampus: a microdialysis study in freely moving rats. Eur J Neurosci 11:2465–2473.

Wyss JM, Swanson LW, Cowan WM (1979) A study of subcortical afferents to the hippocampal formation in the rat. Neuroscience 4:463–476.

Xia M, Wang J, He Y (2013) BrainNet viewer: a network visualization tool for human brain connectomics. PloS One 8:e68910.

Xi G, Hui J, Zhang Z, Liu S, Zhang X, Teng G, Chan KC, Wu EX, Nie B, Shan B, Li L, Reynolds GP (2011) Learning and memory alterations are associated with hippocampal *N*-acetylaspartate in a rat model of depression as measured by 1H-MRS. PloS One 6:e28686.

Xin L, Tkáč I (2017) A practical guide to *in vivo* proton magnetic resonance spectroscopy at high magnetic fields. Analyt Biochem 529:30–39.

Yang CH, Huang CC, Hsu KS (2005) Behavioral stress enhances hippocampal CA1 long-term depression through the blockade of the glutamate uptake. J Neurosci 25:4288–4293.

Yang Z, LaConte S, Weng X, Hu X (2008) Ranking and averaging independent component analysis by reproducibility (RAICAR). Hum Brain Mapp 29:711–725.